ELSEVIER

Journal of Nuclear Materials 252 (1998) 257–265

journal of nuclear materials

Dynamic strain aging sensitivity of heat affected zones in C–Mn steels

D. Wagner *, J.C. Moreno, C. Prioul

Laboratoire MSS / MAT, CNRS URA 850, Ecole Centrale de Paris, 92295 Chatenay Malabry cedex, France

Received 21 August 1997; accepted 10 September 1997

Abstract

In weakly killed C–Mn steels, the dynamic strain aging (DSA) phenomenon induces an increase in the ultimate tensile strength associated with a ductility loss, usually measured in the 100–200°C temperature range. This phenomenon, which induces large toughness reductions, is not well characterized in the heat affected zones (HAZ) of the welds, since the sensitivity to DSA cannot be directly determined due to the very abrupt microstructure gradients existing in these zones. In order to study the influence of microstructure on DSA, tensile tests were performed on simulated HAZ, resulting from various quenching conditions of C–Mn steels. These results are interpreted through correlations with internal friction results on the same microstructures. It is concluded that the materials which have been submitted to the more severe quenching conditions appear to be less sensitive to DSA. This trend is attributed to the larger density of dislocations which can trap most of the interstitial atoms in these microstructures. Whatever the microstructure, the intensity of DSA, characterized by the ductility loss, is proportional to the Snoek peak height measured by internal friction. This result allows the evaluation of the sensitivity of C–Mn steels to DSA from a unique internal friction test. © 1998 Elsevier Science B.V.

1. Introduction

Carbon–manganese steels, in the form of pipes, plates and forgings, and associated welds are commonly used for pressurized water reactors secondary systems (feedwater line and steam line). Nevertheless, if they are insufficiently killed, these steels are well known to be sensitive to dynamic strain aging (DSA). This phenomenon, which is observed in metals containing solute atoms interacting with dislocations [1–3], induces an increase in flow stress, ultimate tensile strengh and work hardening coefficient, as well as a decrease in ductility (elongation, reduction of area and fracture toughness). Dynamic strain aging produces various types of inhomogeneous deformations labelled as Portevin-le-Chatelier effect (PLC) [4], observed in a temperature range which is clearly dependent on the mobility of the solute atoms, relative to the imposed dislocation velocity [5–10].

In C–Mn steels, it is well established [1] that the diffusing species are interstitial carbon and nitrogen atoms. Moreover, according to its greater solubility limit [11,12], nitrogen content seems to exert a more pronounced influence on strain aging than carbon content does. Depending on the diffusion coefficients, the chemical composition of the steels and the strain rate, the temperature where DSA occurs varies from 200 to 350°C [1–3], in coincidence with the operating temperature range of the secondary lines of pressurized water reactors (PWR).

Due to its strong potential nocivity, DSA, which induces large toughness reductions, has been extensively studied in base C–Mn metals. Nevertheless, it is not well characterized in the heat affected zones (HAZ) of the welds, since the sensitivity to DSA cannot be directly determined, due to the very abrupt microstructure gradients existing in these zones. To ensure better structural integrity of welded joints, a thorough characterization of HAZ sensitivity to DSA is therefore needed.

Few investigations of the influence of microstructures on DSA are reported in steels. The influence of microstructure on static strain aging (SSA) and DSA was studied by

* Corresponding author. Fax: +33-1 41 13 14 30.

PII S0022-3115(97)00279-1

Table 1
A48 steel chemical composition (wt%)

C	S	P	Si	Mn	Ni	Cr	Mo
0.198	0.012	0.0104	0.207	0.769	0.135	0.095	0.025
V	Cu	Sn	Al	N	O	Ti	Nb
< 0.003	0.273	0.023	0.004	0.0083	0.0049	< 0.003	< 0.004

Chakravartty et al. [13,14] in a low alloyed nickel–manganese steel (A 203 D containing 0.13 wt% C, 0.52% Mn, 3.43% Ni, 48 ppm N and less than 0.01% Al). From tensile tests and strain rate sensitivity measurements performed in the 25 to 250°C temperature range on various cold worked and aged microstructures (as quenched or tempered martensite, ferrite and pearlite) these authors concluded that no microstructure dependence on the SSA and DSA sensitivity could be observed in this alloy.

The objective of the present study is to compare the DSA sensitivity of different simulated heat affected zones realized by thermal treatment of a C–Mn steel. The DSA sensitivity has been characterized from an engineering point of view, as the ductility loss or the ultimate tensile strength increase deduced from tensile tests. The internal friction technique has been employed considering its capacity to evaluate the balance between free carbon or nitrogen atoms in the lattice and carbon or nitrogen atoms interacting with mobile dislocations. This correlation between internal friction experiments and tensile tests offers new insights for a better understanding of the phenomena.

2. Materials and experimental techniques

2.1. Materials

The material used in this study is a carbon–manganese steel of AFNOR (French standard) NFA 36205 grade A48 which was received as a 40 mm thick plate. The chemical composition, which is reported in Table 1, corresponds to that of a silicon semi-killed steel containing very little aluminium that can trap nitrogen atoms by aluminium nitride (AlN) formation. Consequently, in this alloy, free nitrogen atoms still present in the lattice can contribute to DSA.

Four blocks (100 mm width, 160 mm long and 40 mm thick) were taken from the original plate (which was normalized at 870°C followed by air cooling). This initial normalized microstructure (labelled as reference in the following) was preserved in one block (block 1), and consisted of banded ferrite and pearlite (Fig. 1). The three other blocks were reaustenized during a total time of about 1 h at different temperatures (1250°C, 1050°C, 900°C) and water quenched, in order to produce different microstructures as close as possible to those existing in the heat affected zones of welds.

In these four blocks, conventional through thickness micrographic observations (Figs. 1–4) were made from polished sections cut along the longitudinal direction, at 40 mm from the block side. In block 2, which was austenized at 1250°C and water quenched, the microstructure consisted of martensite, bainite and ferrite (Fig. 2). No difference could be detected between half and quarter thickness

Fig. 1. Microstructure of normalized air cooled block 1 (reference).

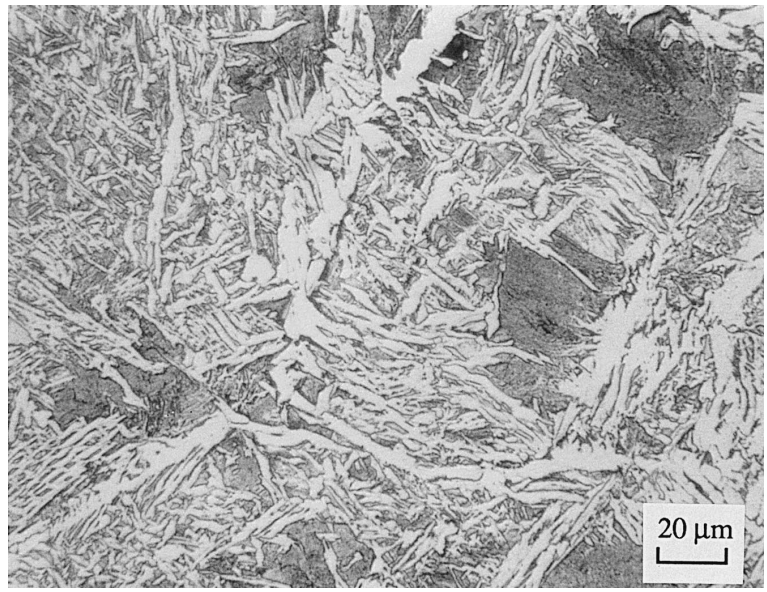

Fig. 2. Microstructure of austenized 1250°C water quenched block 2.

observations. In block 3, which was austenized at 1050°C and water quenched, the microstructure also consisted of martensite, bainite and ferrite (Fig. 3), but finer grains than in block 2 can be observed. The different proeutectoid ferrite distribution, which is more acicular in block 2, is due to the better homogenization of the austenite chemical composition during the 1250°C thermal treatment. In block 3, slight microstructure differences can be observed between quarter and mid thickness with a more quenched and finer microstructure in the mid section. In block 4, which was austenized at 900°C and water quenched, a banded microstructure consisting of bainite, ferrite and degenerated pearlite was obtained (Fig. 4).

2.2. Tensile tests

Tensile tests were carried out in the 20–300°C temperature range on an Instron screw driven machine with a

Fig. 3. Microstructure of austenized 1050°C water quenched block 3.

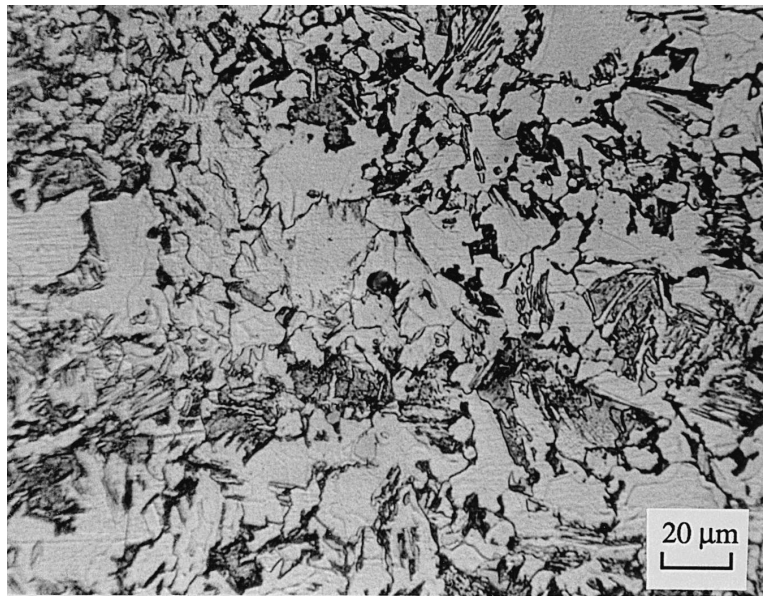

Fig. 4. Microstructure of austenized 950°C water quenched block 4.

strain rate of 2.4×10^{-4} s^{-1}. Cylindrical specimens (4 mm diameter) were machined in the quarter thickness longitudinal direction of the plates. Conventional and true stress–strain curves were plotted. The yield strength, σ_{YS}, the ultimate tensile strength, σ_{UTS}, the uniform and total elongation, the reduction of area as well as the work hardening coefficient were determined versus temperature.

2.3. Internal friction experiments

Internal friction experiments were performed in the -20 to 300°C temperature range on an inverted torsion pendulum [15] with an applied strain of 5×10^{-6} and a heating rate of 130°C per hour. The samples (3 mm diameter, 50 mm gage length) were also machined in the quarter thickness transverse direction of the plates. This sample geometry leads to a resonant frequency of the apparatus which is close to 1.5 Hz. Three metallurgical conditions were tested: normalized (reference block 1), austenized at 1250°C (block 2) or 1050°C (block 3). Furthermore, one test was performed on the normalized microstructure, after 8% cold working and one month room temperature aging.

3. Experimental results

3.1. Tensile tests

In the normalized material, whatever the temperature, a Lüders plateau is observed on the conventional tensile curves (nominal stress versus elongation ($\Delta L/L_0$)). The Portevin-le-Chatelier (PLC) phenomenon is clearly exhibited at both 100 and 200°C. Nevertheless, whereas typical serrated yielding is observed at 200°C, the phenomenon is less pronounced at 100°C, leading to less periodic serrations (irregular PLC). In the reaustenized materials the Lüders plateau is never observed and only irregular PLC phenomenon appears at 100°C.

The variations of the yield strength, σ_{YS}, the ultimate tensile strength, σ_{UTS}, the uniform and total elongations, as well as the reduction of area are plotted versus temperature in Figs. 5–9, for the four metallurgical conditions. In the temperature range tested, all the microstructures display yield stress and ultimate tensile stress maxima associ-

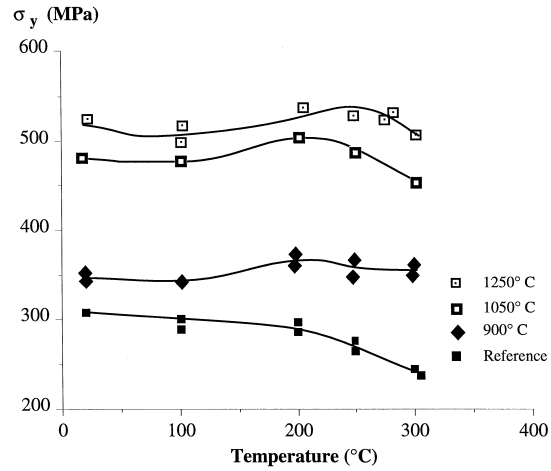

Fig. 5. σ_{YS} variation with temperature.

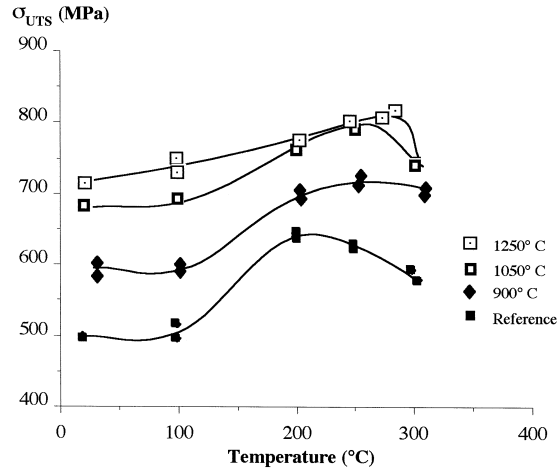

Fig. 6. σ_{UTS} variation with temperature.

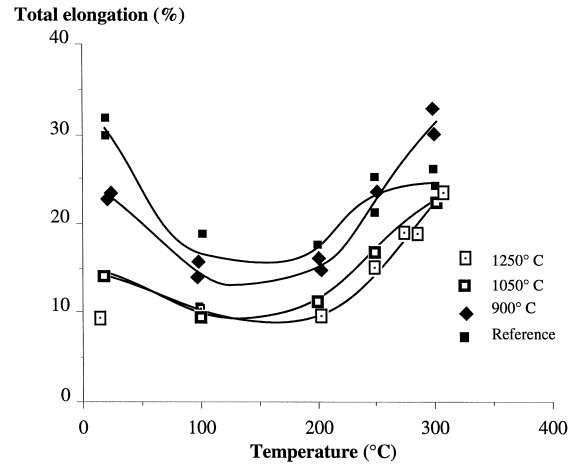

Fig. 8. Total elongation variation with temperature.

ated with elongation and reduction of area minima which are characteristics of the DSA phenomenon. In the normalized steel the σ_{UTS} maximum and the corresponding minimum in reduction of area occur at 200°C. These extrema are shifted to 250°C in reaustenized materials, although the DSA starting temperature (temperature where σ_{UTS} begins to increase) is the same. The total and uniform elongations go through a minimum but, whatever the metallurgical state, these minima appear at lower temperatures (100–200°C) than the strength maxima.

From a $\sigma = k\varepsilon^n$ fitting of the true stress versus true strain curves, the variations of the strain hardening coefficient n have been plotted versus temperature for the different microstructures (Fig. 10). This figure shows that the harder the microstructure is, the lower is the strain hardening coefficient measured at room temperature and the lower is the increase with temperature. Furthermore, in the normalized state, n reaches a maximum at 200°C.

3.2. Internal friction results

The internal friction spectrum measured in the normalized microstructure reveals two main peaks in the −20 to 300°C temperature range (Fig. 11, curve 1). The first one which presents a maximum at about 20°C can be associated with the Snoek peak (SP) resulting from carbon and nitrogen redistribution between octahedral sites in the ferritic or martensitic lattice. Due to complex interactions between nitrogen and manganese, which will be discussed further on, the Snoek peak height is not directly proportional to C and N interstitial content in the lattice, as observed in pure iron. The second peak, observed in the 150–250°C temperature range, corresponds to the cold work peak (CWP) and is due to the interaction between dislocations and interstitials such as carbon and nitrogen. The CWP height is related to both the density of mobile dislocations and the interstitial content in the vicinity of

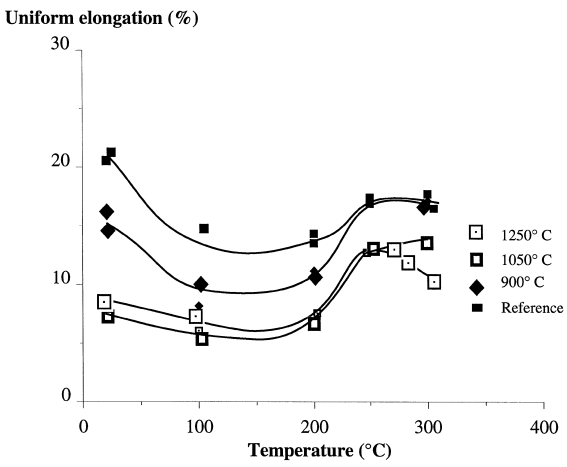

Fig. 7. Uniform elongation variation with temperature.

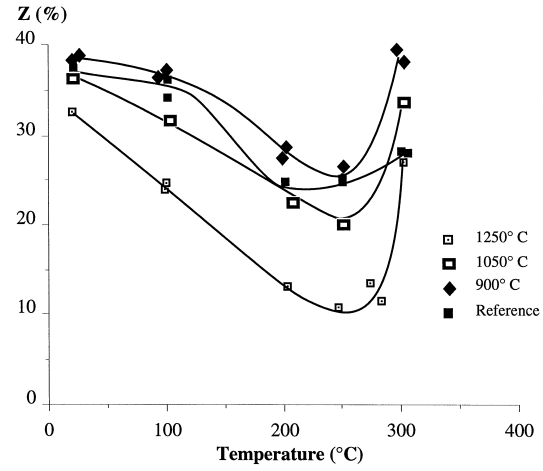

Fig. 9. Reduction of area variation with temperature.

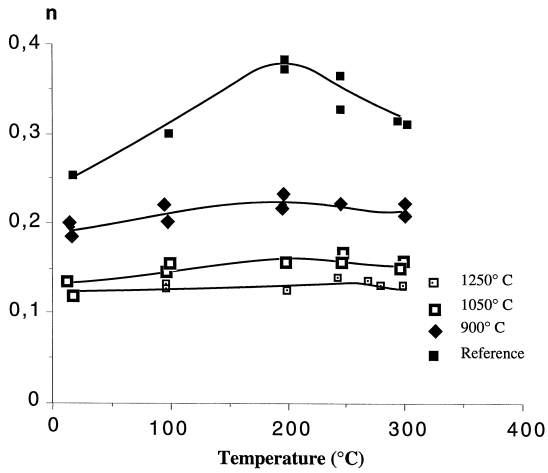

Fig. 10. Work hardening rate variation with temperature.

dislocations. This classical interpretation of the internal friction spectrum in steels is confirmed by curve 2 which represents the internal friction variation measured in the normalized microstructure, after 8% cold working and one month room temperature aging. In that case, an increase of the CWP with dislocation density is observed, associated with a corresponding SP decrease, in agreement with the classical balance of interstitial atoms between lattice and dislocations [36].

The internal friction plots obtained in quenched microstructures (tested after 3 months room temperature aging) are also reported in Fig. 11 (curves 3 and 4). The comparison between all these plots reveals that the SP decreases whereas the CWP increases, either after quenching, or cold working. More pronounced modifications are observed after quenching.

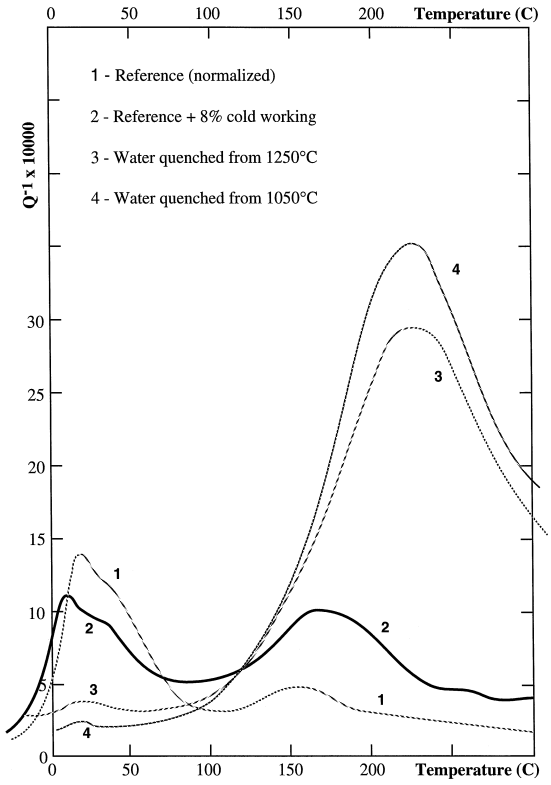

Fig. 11. Internal friction plot.

4. Discussion

4.1. Tensile tests

From Figs. 5–10 it appears that the dynamic strain aging phenomenon is clearly evidenced in all the microstructures tested, especially by the jerky flow observation and associated ductility loss on the stress–strain curves. In the temperature range tested, a larger evolution of the different parameters is always observed in the normalized (reference) microstructure. For instance, in this microstructure, the maximum ultimate tensile stress is 140 MPa higher than the room temperature value whereas only an 80 MPa increase is measured in the materials austenized at 1250°C and quenched. Correspondingly, in comparison with the room temperature value, a 14% drop of the total elongation is observed in the normalized (reference) microstructure whereas it is limited to 3% in the 1250°C austenized and quenched microstructure. From this point of view, the hardest microstructures, consisting mainly of martensite, bainite and ferrite appear to be less sensitive to DSA. This lower sensitivity of quenched microstructures is in good agreement with the less pronounced PLC effect, observed on the tensile curves of the hardest microstructures.

4.2. Internal friction tests

For steels with carbon content below 0.25%, the martensite is cubic [16]. In the present steel, according to the formula $c/a = 1000 + 0.045$ wt% C, the difference between c and a lattice parameters is lower than 1%, so the carbon and nitrogen atoms can be considered as randomly distributed between the octahedral sites, each octahedral site keeping its original spherical symmetry. This makes no differentiation between the relaxation phenomena observed in both ferrite or low carbon martensite.

As shown in Fig. 11, the Snoek peak, due to free carbon and nitrogen redistribution between equivalent octahedral sites in the lattice, which appears at 20°C, reveals a more complex shape than in pure iron. As discussed by Koiwa [17], the SP disymmetry in these industrial materi-

als results from the overlapping of C peak (located around 39°C in α-Fe, [18,19]) and N peak (around 24–25°C in α-Fe, [18–20]) and essentially from the presence of substitutional manganese, which modifies the jump process of nitrogen atoms.

The cold work peak (also known as Snoek–Köster peak) observed between 150 and 200°C is due to mobility of the interstitial atoms in the dislocations stress field. The exact mechanism of this relaxation is still controversial [21,22]. In the more simple model, the dislocation line pinned in two points, drags solute atoms as it bows out under the oscillating stress. At low temperature, interstitial atoms mobility is not sufficient to follow dislocations, whereas at high temperature, this mobility is too important and, in both cases, no energy dissipation is involved. At intermediate temperatures, the dragging of the interstitial atoms by the dislocations is effective and results in the energy loss measured by internal friction.

Room temperature aging and tempering of Fe–C and Fe–C–N have been studied extensively by many authors, in various microstructures, including supersaturated water-quenched ferrite [23,24] and martensites of Fe–N [25], Fe–C [26], Fe–C–N [27]. From these studies it appears that, after room temperature aging, the interstitial atoms are distributed through various sites:

– most of the nitrogen and carbon atoms are clustered in local enriched zones which, after a sufficient time, lead (in Fe–N and Fe–C ferrites) to $\alpha''Fe_{16}N_2$ or $Fe_{16}(C,N)_2$ carbonitrides precipitation;

– a noticeable part of interstitial atoms are trapped in the vicinity of lattice defects such as dislocations;

– the remaining part of the interstitial atoms are randomly distributed between the octahedral sites of the solid solution. Internal friction results by Fergusson and Jack [23] showed that these atoms contribute to the Snoek peak observed in these structures. Therefore, the peak height can give a measure of the nitrogen (and carbon) content in the lattice.

The distribution of C and N atoms between these different sites (clusters, lattice defects and solid solution) is strongly dependent on defect density relative to nitrogen and carbon content. In freshly quenched Fe–Ni–C martensites (with a 5×10^{11} cm^{-2} dislocation density), Wyslich et al. [28] have evaluated the amount of carbon atoms segregating on lattice defects during aging, for various carbon contents. For 0.8% C, they have shown that nearly 67% of the carbon atoms are trapped in the dislocations stress field whereas this amount reaches 80% in Fe–Ni 0.4% C and 83.5% in Fe–Ni 0.2% C. Similar results have been given by Nishiyama [29] in Fe–C martensite, with less than 0.2% C. In that case, due to the higher M_S temperature, interstitial redistribution can occur during both quenching and further aging, and it can be estimated that 90% of the carbon atoms have clustered on lattice defects [29], thus partly explaining why martensite remains cubic in low carbon steels.

In low carbon martensite, with lath morphology, the very high dislocation density observed [30–32] is difficult to quantify exactly but the order of magnitude is close to 10^{12} cm^{-2} [2,33], whereas it is much lower (10^8 or 10^9 cm^{-2}) in low carbon ferritic steels [2,34].

Assuming that the linear relationship between Snoek peak height and free interstitial atoms content is the same in the ferritic and in the martensitic phase (according to the cubic crystallography of low carbon martensites), the internal friction plot reported in Fig. 11 for different microstructures of the same C–Mn steel (0.2 C and 80 ppm N) can be interpreted as follows. In the normalized microstructure, the low density of dislocations, confirmed by the existence of a small cold work peak (CWP), offers few sites for the trapping of interstitial atoms on dislocations. Consequently, carbon and nitrogen atoms occupy preferentially the octahedral sites of the lattice, in agreement with the large Snoek peak observed. At the opposite, in the quenched microstructures, due to the strong interaction of interstitial atoms with the high density of dislocations in martensite (exhibited by the large CWP), only few C and N atoms are still present in the solid solution, as demonstrated by the small Snoek peak observed in these structures. In order to confirm this balance between free interstitial atoms in the lattice and interstitial atoms trapped on dislocations, a normalized sample has been 8% cold worked and aged (1 month) at room temperature. After Baird [1], this one month aging at room temperature allows nitrogen diffusion over a distance of 6×10^{-6} cm which is the mean distance between dislocations in cold worked iron. Such an aging procedure leads to dislocation sites filling by C and N atoms. Fig. 11 (curve 2) confirms the Snoek peak decrease and the corresponding CWP increase, in agreement with the usual effect of cold working on Snoek peak height [22]. In agreement with the lower density of dislocations attainable by cold working, relative to that associated to martensitic transformation, the internal friction plot (Fig. 11, curve 2) is intermediate between the evolutions of normalized (curve 1) and quenched microstructures (curves 3 and 4).

4.3. Correlation between internal friction and tensile tests results

In pure bcc metals, the Snoek peak height is proportional to C or N atoms in solid solution. Nevertheless, in steels the Snoek peak is more complex, due to overlapping of C and N peaks and also to nitrogen Snoek peak distortion by nitrogen–manganese interaction [17]. In this case the deconvolution of the different peaks is doubtful and the quantitative determination of free C and N content in the lattice is not reliable. We have therefore plotted on Figs. 12 and 13 the global Snoek peak height versus two different DSA sensitivity parameters defined considering an engineering point of view. The first one, $((\Delta L/L_0)_{20°C} - (\Delta L/L_0)_{min})/(\Delta L/L_0)_{20°C}$, corresponds to the loss in

total elongation over the temperature range tested, relative to the total elongation measured at 20°C. The second one, $((UTS)_{max} - (UTS)_{20°C})/(UTS)_{20°C}$, corresponds to the relative increase of the ultimate tensile strength. As reported in Figs. 12 and 13, a linear relationship can be plotted between the Snoek peak height and these two DSA sensitivity indexes defined above. On these figures additional results, previously reported [35], and concerning an A42 steel and a deposited manual metal arc weld (MMAW), having manganese contents similar to that in the steel tested, are also included. Further experiments (not reported here) realized on different steels with various manganese content have shown that no unique linear correlation can be plotted between DSA sensitivity and Snoek peak height. This influence of manganese content can be interpreted in terms of the strong interaction existing between nitrogen and manganese, as illustrated by the large nitrogen Snoek peak modification by manganese reported by different authors in nitrogen steels [17,36,37]. Furthermore, the weak DSA observed on Figs. 12 and 13, in the absence of any corresponding Snoek peak, can be attributed partly to the insufficient resolution of our internal friction measurements, since only a few ppm of nitrogen atoms are needed to give rise to DSA [38]. It must also be considered that internal friction tests are conducted on microstructures which are nearly in equilibrium at the considered temperature, whereas the plastic deformation during tensile tests leads probably to partial C and N redistribution from dislocations sites to interstitial sites of the lattice. This interstitial redistribution accompanying tensile tests can give rise to DSA phenomena which are not observable by internal friction measurements on the initial microstructure.

The correlation which has been established between Snoek peak height and DSA sensitivity indicates that DSA

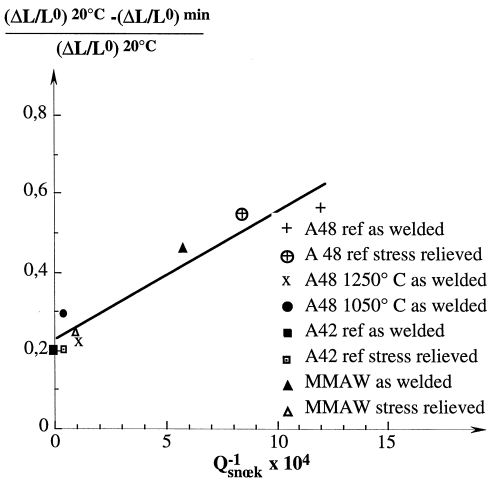

Fig. 12. Elongation DSA sensitivity index versus Snoek peak height.

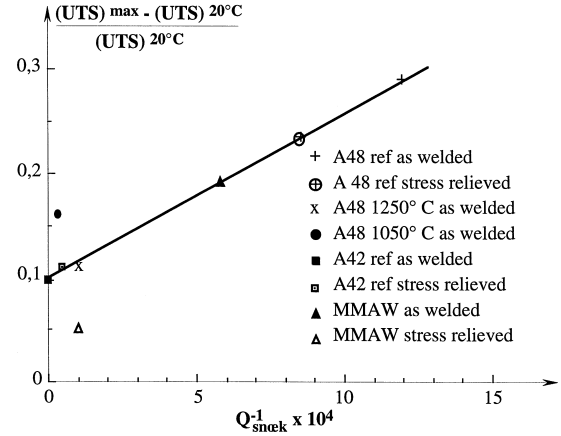

Fig. 13. UTS DSA sensitivity index versus Snoek peak height.

is directly governed by the amount of free interstitial nitrogen and carbon atoms in the lattice. As shown by the internal friction experiments, this free interstitial content is strongly microstructure dependent. The lower sensitivity to DSA reported in the quenched microstructures, consisting of martensite, bainite and ferrite can be attributed to C and N trapping on the dislocations resulting from the quenching procedure and revealed by the CWP increase associated to Snoek peak weakening. This strong influence of dislocation density on free interstitial trapping by room temperature aging is clearly emphasized by the evolution reported in cold worked microstructures, as compared with those reported in the initial normalized microstructures (Fig. 11).

A comparison between the variations of the different tensile test parameters reported versus temperature in Figs. 7–9, shows that the influence of DSA is shifted to higher temperatures when the austenizing temperature is increased. Similar results (not reported) have been obtained in C–Mn welds with different amount of manganese. This trend can tentatively be attributed to the increasing manganese content of the lattice, resulting from higher austenizing temperatures and, as mentioned above, at a strong Mn/N interaction which leads to a reduced mobility of nitrogen atoms. Consequently, in the presence of high Mn content in the lattice, DSA phenomenon extends to higher temperatures. Further experiments would be needed to confirm this interpretation.

5. Conclusion

In order to characterize the sensitivity of C–Mn steel weld HAZ to dynamic strain aging, the influence of microstructure has been studied by tensile and internal friction tests on simulated heat affected zones. These microstructures were obtained by water quenching after varying the austenizing temperature in the 900 to 1250°C

temperature range. The following conclusions can be drawn:

– the DSA phenomenon is shown to be strongly microstructure dependent. The more severely quenched microstructures, consisting of martensite, bainite and ferrite are less sensitive to DSA. This lower sensitivity to DSA can be attributed to the C and N trapping on the dislocations resulting from the quenching procedure as revealed by the internal friction cold work peak increase and Snoek peak decrease;

– the DSA sensitivity, evaluated by the ductility loss or the UTS increase, is proportional to Snoek peak height. This important result shows that even in industrial materials a single internal friction test can give a precise evaluation of DSA sensitivity.

Acknowledgements

The financial support of FRAMATOME is greatly acknowledged. Thanks are due to MM Houssin, Faure and Meyzaud for fruitful discussions and for providing the C–Mn steels for this study.

References

[1] J.D. Baird, Strain aging of steel — a critical review, Iron and Steels, May 1963, pp. 186, 326, 368, 400 and 450.
[2] J.D. Baird, Dynamic Strain Aging in the Inhomogeneity of Plastic Deformation, ASM, Metals Park, OH, 1973, p. 191.
[3] A.S. Keh, Y. Nakada, W.C. Leslie, Dynamic Strain Aging in Iron and Steel in Dislocation Dynamics, McGraw-Hill, New York, 1968, p. 381.
[4] P. Lacombe, Matériaux et Techniques, Aug.–Sept. 1985, E5.
[5] A.H. Cottrell, Dislocations and Plastic flow in Crystals, Clarendon, Oxford, 1953.
[6] P.G. McCormick, Acta Metall. 20 (1972) 35.
[7] A. Van den Beukel, Phys. Status Solidi 30 (1975) 197.
[8] A.W. Sleeswijk, Acta Metall. 6 (1958) 598.
[9] R.A. Mulford, U.F. Kocks, Acta Metall. 27 (1979) 1125.
[10] L.P. Kubin, Y. Estrin, J. Phys. III 1 (1991) 929.
[11] W.C. Leslie, Quench and Strain Aging in Encyclopedia of Materials Science and Engineering, vol. 5, Pergamon, Oxford, UK, 1986, p. 4007.
[12] C.W. Marschall, M.P. Landow, G.M. Wilkowski, ASTM STP 1074, ASTM, Philadelphia, 1990, p. 339.
[13] J.K. Chakravartty, A. Haq, T.K. Sinha, M.K. Asundi, Trans. Ind. Inst. Met. 37 (5) (1984) 501.
[14] J.K. Chakravartty, S.L. Wadekar, T.K. Sinha, M.K. Asundi, J. Nucl. Mater. 119 (1983) 51.
[15] C. Prioul, M. Pasquet, M. Carrard, J. Plusquellec, P. Azou, Mem. Et. Sci. Rev. Met. 79 (1982) 203.
[16] Z. Nishiyama, Crystallography of Martensite in Martensitic Transformation, Academic Press, London, 1978, p. 17.
[17] M. Koiwa, Philos. Mag. 24 (1971) 81.
[18] A.E. Lord, D.N. Beshers, Acta Metall. 14 (1966) 1659.
[19] J.R.G. da Silva, R.B. McLellan, Mater. Sci. Eng. 26 (1976) 83.
[20] I.G. Ritchie, R. Rawlings, Acta Metall. 15 (1967) 491.
[21] G. Schœck, Scripta Metall. 22 (1988) 389.
[22] T.S. Kê, Scripta Metall. 16 (1982) 225.
[23] P. Fergusson, K.H. Jack, Proc. Heat Treatment Conf., Metals Soc., Birmingham, 1981, p. 158.
[24] R. Borrely, D. Benkirat, Acta Metall. 33 (5) (1985) 855.
[25] L. Cheng, N.M. Van der Pers, A. Bottger, Th.H. De Keijser, E.J. Mittemeijer, Metall. Trans. A 21 (1990) 2857.
[26] L. Cheng, N.M. Van der Pers, A. Bottger, Th.H. De Keijser, E.J. Mittemeijer, Metall. Trans. A 22 (1991) 1957.
[27] L. Cheng, A. Bottger, E.J. Mittemeijer, Metell. Trans. A 23 (1992) 2737.
[28] P. Wyslich et al., Konove Mater. 1 (1976) 18.
[29] Z. Nishiyama, Crystallography of Martensite in Martensitic Transformation, Academic Press, London, 1978, p. 163.
[30] C.M. Wayman, Martensitic Transformations, TransTech, Aedermannsdorf, 1989, pp. 1–32.
[31] C.M. Wayman, Physical Metallurgy, North Holland, Amsterdam, 1983, p. 1045.
[32] Y.H. Tan et al., Metell. Trans. A 23 (1992) 1413.
[33] G. Krauss, Trait. Thermique 201 (1986) 15.
[34] H.J. Klaar, P. Schwaab, W. Osterle, Prakt. Metallogr. 29 (1992) 3.
[35] D. Wagner, C. Prioul, D. François, J. Alloys Comp. 211&212 (1994) 132.
[36] J.D. Fast, Mét. Cor. Ind. 435 (1961) 383.
[37] I.A. Tomilin, M.N. Churyukanova, Steel USSR 17 (1987) 43.
[38] M. Grumbach, G. Sanz, CIT 5 (1970) 1285.